

Photo-assisted electrochemical etching of high-Al-content AlGaN sacrificial layers for UVC applications

Downloaded from: https://research.chalmers.se, 2026-11-22 23:58 UTC

Citation for the original published paper (version of record):
Nguyen, T., Shushanian, A., Kowallik, V. et al (2026). Photo-assisted electrochemical etching of high-Al-content AlGaN sacrificial layers for UVC applications. Journal of Applied Physics, 140(16). http://dx.doi.org/10.1063/5.0353096

N.B. When citing this work, cite the original published paper.

research.chalmers.se offers the possibility of retrieving research publications produced at Chalmers University of Technology. It covers all kind of research output: articles, dissertations, conference papers, reports etc. since 2004. research.chalmers.se is administrated and maintained by Chalmers Library

(article starts on next page)

Journal of Applied Physics

RESEARCH ARTICLE | OCTOBER 29 2026

Photo-assisted electrochemical etching of high-Al-content AlGaN sacrificial layers for UVC applications

Thanh Phuc Nguyen ; Artem Shushanian ; Verena Kowallik ; Ryan Page ; Tim Wernicke ; Michael Kneissl ; Joachim Ciers ; Åsa Haglund

Check for updates

J. Appl. Phys. 140, 165706 (2026)
https://doi.org/10.1063/5.0353096

View Online Export Citation

Articles You May Be Interested In

Electrochemical porosification of n-GaN across acidic–neutral–alkaline electrolytes: From morphology to surface chemistry

J. Chem. Phys. (July 2026)

Activation study on Ge-implanted gallium nitride and its usage in dopant-selective nanoporous electrochemical etching

J. Appl. Phys. (July 2026)

The impact of dislocation-mediated etching on the structure of porous GaN

J. Appl. Phys. (May 2026)

16 November 2026 08:04:57

Nanotechnology & Materials Science | Optics & Photonics | Impedance Analysis | Scanning Probe Microscopy | Sensors | Failure Analysis & Semiconductors

Unlock the Full Spectrum.
From DC to 8.5 GHz.



Zurich Instruments

Find out more

AIP Publishing

Journal of Applied Physics ARTICLE pubs.aip.org/aip/jap

Photo-assisted electrochemical etching of high-Al-content AlGaN sacrificial layers for UVC applications

Cite as: J. Appl. Phys. **140**, 165706 (2026); doi: 10.1063/5.0353096
Submitted: 20 July 2026 · Accepted: 9 October 2026 ·
Published Online: 29 October 2026

View Online Export Citation CrossMark

Thanh Phuc Nguyen,[1,a)] Artem Shushanian,[1] Verena Kowallik,[2] Ryan Page,[1] Tim Wernicke,[2] Michael Kneissl,[2,3] Joachim Ciers,[1] and Åsa Haglund[1]

AFFILIATIONS

[1]Department of Microtechnology and Nanoscience, Chalmers University of Technology, 41296 Gothenburg, Sweden
[2]Institute for Physics and Astronomy, Technische Universität Berlin, 10623 Berlin, Germany
[3]Ferdinand-Braun-Institut (FBH), 12489 Berlin, Germany

[a)]**Author to whom correspondence should be addressed:** phuc@chalmers.se

ABSTRACT

Selective etching of $Al_xGa_{1-x}N$ with $x > 0.5$, e.g., for the substrate lift-off of UVC emitters, is extremely challenging due to the very high bonding strength of the compound. Even electrochemical etching (ECE), which has proven very effective in $Al_xGa_{1-x}N$ with lower x, leads to porosification rather than complete etching. We show here that by adding illumination during etching, i.e., photo-assisted electrochemical etching (P-ECE), complete etching can be achieved for x up to 65%. We studied the P-ECE of a range of sacrificial layers consisting of a highly Si-doped ($[Si] = 3 \times 10^{19}$ cm^{-3}) multilayer AlGaN sacrificial layer of five periods of 5 nm $Al_xGa_{1-x}N$/5 nm $Al_yGa_{1-y}N$, with Al content (x/y) between (38%/48%) and (65%/75%) to lift-off $Al_{0.76}Ga_{0.24}N$ membranes. The etching behavior was studied by varying the applied bias voltage, illumination intensity, and excitation wavelength of the photoexcitation source. The N-polar surface of a membrane grown on those multilayer sacrificial layers had a root-mean-square surface roughness between 5.9 and 7.8 nm, with a $5 \times 5\,\mu m^2$ scan size. By using a single 10 nm-thin sacrificial layer instead, we could obtain even smoother etched surfaces with a roughness of below 3 nm, comparable to that of the as-grown surface. We, thus, show that P-ECE is a promising technique for lifting off AlGaN membranes with high Al content and obtaining accurate control of the membrane thickness.

© 2026 Author(s). All article content, except where otherwise noted, is licensed under a Creative Commons Attribution (CC BY) license (https://creativecommons.org/licenses/by/4.0/). https://doi.org/10.1063/5.0353096

I. INTRODUCTION

Substrate removal of ultraviolet (UV) AlGaN-based emitter devices allows for the realization of exciting new device concepts that require optical and electrical access to both sides of the semiconductor layer. In this way, microcavities can be formed to fabricate resonant-cavity light-emitting diodes (RCLEDs)[1] and vertical-cavity surface-emitting lasers (VCSELs).[2–5] Furthermore, this technique allows the transition from conventional lateral current spreading to vertical current injection schemes, reducing current crowding and series resistance, as well as improving heat dissipation and light extraction efficiency.[6–11]

The substrate removal process in UV AlGaN-based emitter devices should ideally preserve the epitaxial structure and exhibit high thickness accuracy combined with a minimal surface roughness. Most techniques can be summarized as either the gradual removal of the substrate or the separation of the layer from the substrate using a sacrificial layer. The former can be achieved through mechanical grinding,[12] polishing with wet chemical treatment,[13,14] and plasma etching.[15,16] The latter approach uses a sacrificial layer, composed of either the same or a different material system, which can be selectively removed by methods such as laser-induced lift-off (LLO),[6,8–10,17–19] water lift-off (WLO),[11,20–22] and electrochemical etching (ECE).[4,23] In addition, another potential substrate removal technique is remote epitaxy using h-BN or graphene as a sacrificial interlayer. This is, however, in the early stage of development, and to the best of our knowledge, only bulk

16 November 2026 08:04:57

© Author(s) 2026

AlN layers have been lifted off, and no functional thin-film AlGaN-based UV emitters have yet been reported.[24–26] Table I summarizes substrate removal methods specifically using an AlGaN-based sacrificial layer.

LLO relies on a sacrificial layer with high optical absorption and a low decomposition temperature. Under external photoexcitation, the sacrificial layer heats up and decomposes. LLO is widely used for GaN-based devices grown on a sapphire substrate.[29] However, the use of a GaN sacrificial layer in general decreases the crystalline quality of higher Al-content epitaxial layers due to the lattice mismatch.[30] To overcome this limitation while maintaining the advantage of the GaN-based sacrificial layer, Wang *et al.* used an AlGaN decoupling structure on a GaN/sapphire template, achieving wafer-scale substrate removal for UV LED devices.[31] However, because this approach still relies on GaN as the release layer, it does not offer as good lattice compatibility with the overgrown AlGaN epilayers, as first demonstrated using an AlN/AlGaN short-period superlattice structure.[8] However, AlGaN layers are more difficult to release at a wafer level and are prone to cracking.[32] A milestone in LLO for AlGaN-based structures was demonstrated by Okuno *et al.*, using an $Al_{0.89}Ga_{0.11}N$ sacrificial layer with an energy density of 2.3 J cm^{-2} in a 0.7 mm^2-sized device.[27] Another method, WLO, exploits void formation during AlGaN growth from AlN nanopillars on sapphire templates.[20,22] Water vapor introduced under saturated vapor pressure selectively etches the m- and a-planes of AlN nanopillars and AlGaN epitaxial layers, while

TABLE I. Lift-off methods for AlGaN sacrificial layers.

Method	Sacrificial layer structure	Substrate removal conditions	RMS roughness (scan size)	Control of device thickness	Ref.
LLO and chemical treatment	200 nm AlN/$Al_{0.6}Ga_{0.4}N$ superlattice	248 nm KrF laser and chemical-mechanical polishing (CMP)	0.96 nm ($10 \times 10\,\mu m^2$)	Challenging	2 and 3
LLO and chemical treatment	100 nm $Al_{0.55}Ga_{0.45}N$	257 nm laser (4th harmonic oscillation of a solid-state laser at 1028 nm) and CMP	[b]	Challenging	9
LLO and chemical treatment	40 nm $Al_xGa_{1-x}N$, x = (55%, 65%, 89%)	193 nm ArF excimer laser, chemical polishing with mixed acid Al etchant	[b]	Challenging	27
WLO	$Al_{0.68}Ga_{0.32}N$/AlN nanopillar template	Vacuuming to 5.3 kPa and returning to atmospheric pressure, followed by heating to 115 °C and pressurizing at 170 kPa	Very rough[a]	Challenging	20 and 22
WLO	$Al_{0.68}Ga_{0.32}N$/AlN nanopillar template	Room temperature (~26 °C) and atmospheric pressure, followed by CMP smoothing and Cl_2 plasma etch	[b]	Challenging	11
ECE	130 nm $Al_xGa_{1-x}N$, x = (11%, 27%, 39%, 50%)	15–30 V, 0.3 M HNO_3	3.5 nm ($1 \times 1\,\mu m^2$)	Good	23
ECE	130 nm $Al_{0.22}Ga_{0.78}N$ 100 nm $Al_{0.39}Ga_{0.61}N$ with 5 × (5 nm $Al_{0.11}Ga_{0.89}N$/5 nm $Al_{0.39}Ga_{0.61}N$)	30 V, 0.3 M HNO_3	3.9 nm ($5 \times 5\,\mu m^2$) 1.7 nm ($5 \times 5\,\mu m^2$)	Good	28
P-ECE	18 nm $Al_{0.45}Ga_{0.55}N$	15 V, 3 mM HNO_3, 30 mW/cm^2 with a 275 nm LED	2.8 nm ($5 \times 5\,\mu m^2$)	Good	5
P-ECE	5 × (5 nm $Al_xGa_{1-x}N$/5 nm $Al_yGa_{1-y}N$), (x/y) = (38%/48%), (41%/51%), (45%/55%), (55%/65%), and (65%/75%) 10 nm $Al_{0.5}Ga_{0.5}N$ and $Al_{0.6}Ga_{0.4}N$	7.5–25 V, 3 mM HNO_3 0–23 mW/cm^2 with a 275 , 265 , and 255 nm LED	5.9–7.8 nm ($5 \times 5\,\mu m^2$) 2.8–2.9 nm ($5 \times 5\,\mu m^2$)	Good	This work

[a]Root-mean-square (RMS) roughness value is missing; the SEM image of the surface is available.
[b]RMS roughness value and SEM image of the surface are missing.

16 November 2026 08:04:57

© Author(s) 2026

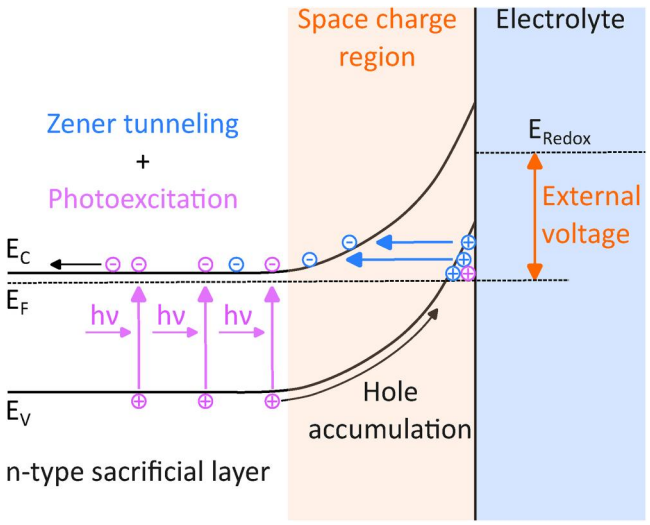

FIG. 1. Illustration of the band diagram of a sacrificial layer/electrolyte junction during photo-assisted electrochemical etching.

oxidation or hydroxylation of the -c-surface forms a brittle altered layer that facilitates exfoliation. WLO, which can also operate at room temperature and atmospheric pressure, offers a promising alternative, although its mechanism is not yet fully understood.[11] Mechanical thinning, LLO, and WLO typically do not yield a smooth surface, which requires post-processing such as chemo-mechanical polishing.[10,11,33] For these methods, controlling device thickness precisely remains a challenge, which is crucial for devices such as VCSELs and RCLEDs, where optical performance is highly sensitive to both cavity thickness and surface roughness.[28,34]

ECE, on the other hand, is a versatile and reliable alternative method for substrate removal, enabling precise control over device thickness while maintaining a low surface roughness. ECE has been applied to realize AlGaN-based devices, including thin-film flip-chip LEDs,[35,36] VCSELs,[28] RCLEDs,[1] high-electron-mobility nano-membrane transistors,[37] micro-resonators,[38] and thin-film UV detectors.[39] The etching selectivity of the sacrificial layer is determined by its Al content and doping concentration of the sacrificial layer in relation to the rest of the device structure, as well as the applied voltage and electrolyte concentration.[40,41] Although the ECE of GaN sacrificial layers has been extensively investigated,[42–44] reports on complete etching of AlGaN sacrificial layers to realize AlGaN membranes remain limited.[1,23,28]

For UVC devices (200–280 nm), the epitaxial device layers contain a higher Al content than those used for UVB devices (280–320 nm), and ideally, the sacrificial layer should then also have a higher Al content to minimize lattice mismatch, especially since UVC structures are grown fully strained to AlN to profit from the reduced dislocation density of AlN substrates[45] or AlN-on-sapphire templates.[46] For such structures with high Al content, the sacrificial layer tends to only porosify instead of etching completely.[23,44] The etching of the sacrificial layer also strongly depends on the template. Bergmann *et al.* showed that an $Al_{0.5}Ga_{0.5}N$ sacrificial layer grown on a relaxed n-doped $Al_{0.5}Ga_{0.5}N$:Si template can be completely etched.[23] However, an $Al_{0.45}Ga_{0.55}N$ layer with the same doping concentration, grown strained to a high-temperature-annealed (HTA) AlN/sapphire, was mostly only porosified, even with a higher applied voltage up to 120 V.[5,47] The mechanism for this discrepancy is not yet fully understood and remains under investigation. Photo-assisted electrochemical etching (P-ECE) offers a potential solution by enhancing the etch rate for high Al contents.[44,48,49] As shown in Fig. 1, applying an external voltage between the electrolyte and the sacrificial layer induces band bending at the semiconductor/electrolyte interface, creating a built-in electric field in the space-charge region. Consequently, electrons can tunnel from the valence band to the conduction band via Zener tunneling, leaving holes behind. With additional photoexcitation, electron-hole pairs are generated, and the built-in electric field drives photoexcited holes toward the sacrificial layer/electrolyte interface, while pushing electrons away. The accumulation of photoexcited holes, together with Zener-generated holes near the interface, promotes oxidation reactions, thereby enabling complete etching of the sacrificial layer.[5,50] However, due to the limited number of studies on P-ECE-based complete etching of AlGaN sacrificial layers, further investigation is needed to enable the effective implementation of this technique. In this work, we demonstrate the first complete P-ECE-based removal of AlGaN sacrificial layers with an Al content of up to 65%, along with a detailed investigation of etching completeness vs illumination conditions and applied voltage. Additionally, we present an approach to reduce the roughness of the etched N-polar surface.

II. EXPERIMENTAL

Figure 2(a) illustrates the AlGaN epitaxial structures used for investigating the P-ECE conditions. We grew the structures using metal-organic vapor phase epitaxy in a $3 \times 2''$ closed-coupled showerhead reactor. Standard precursors, including trimethylaluminum (TMAl), trimethylgallium (TMGa), and ammonia (NH_3), were employed with hydrogen as the carrier gas. Silane (SiH_4) was utilized as the source for n-type doping. The high-temperature-annealed AlN/c-sapphire templates were provided by the Ferdinand-Braun-Institut (FBH), and the growth started with AlN and AlGaN buffer layers. The following 800 nm Si-doped (6×10^{18} cm^{-3}) $Al_{0.76}Ga_{0.24}N$ layer serves as a current-spreading layer for the P-ECE. All Si concentrations were estimated from Si precursor flow during growth. A moderately high doping concentration was chosen for the current-spreading layer to minimize the potential drop across the sample, hence promoting uniform etching, but still low enough to suppress ECE of the current-spreading layer. Then, we grew a 200 nm-thick etch block $Al_{0.76}Ga_{0.24}N$ layer, with a Si-doping concentration of 6×10^{17} cm^{-3}. The etch block layer was designed to focus the etching process primarily in the sacrificial layer, potentially reducing unwanted etching in the current-spreading layer. The Al content in both the current-spreading layer and the etch block layer was selected to minimize absorption of the light enhancing the etching in these layers, yielding a higher generation of photo-excited carriers in the sacrificial layer. Grown on top of it, a multilayer structure with five periods of alternating 5 nm $Al_xGa_{1-x}N$ and 5 nm $Al_yGa_{1-y}N$ served as a sacrificial layer (50 nm in total). The Si-doping concentration of the sacrificial layer was 3×10^{19} cm^{-3},

16 November 2026 08:04:57

© Author(s) 2026

which promotes etching of this layer. The Al contents (x/y) were (38%/48%), (41%/51%), (45%/55%), (55%/65%), and (65%/75%) for different samples. For comparability, the estimated Si concentration of 3×10^{19} cm^{-3} for different Al-content samples was kept constant. However, the free-electron concentration was not experimentally determined and is expected to decrease with increasing Al content, posing challenges for P-ECE in high-Al-content sacrificial layers. In addition, we grew samples with a 10 nm-thin single sacrificial layer of $Al_{0.5}Ga_{0.5}N$ and $Al_{0.6}Ga_{0.4}N$, using the same Si-doping concentration as in the 50 nm sacrificial layer. Finally, a 600 nm unintentionally doped $Al_{0.76}Ga_{0.24}N$ layer (which will be turned into a membrane after complete etching) capped the entire epitaxial structure. The Al composition of the epitaxial layers was verified by x-ray diffraction reciprocal-space mapping.

To investigate the etching process, we created 10 μm-diameter wide access holes by inductively coupled-plasma reactive-ion etching. In the same plasma etching step, we also opened the current-spreading layer to deposit the vanadium-based contact for ECE. Then, a bilayer photoresist was applied to protect almost the entire sample, except for the access holes. The full process flow of our samples is presented in Fig. S1 in the supplementary material. We ran our P-ECE experiments at room temperature using a 3 mM nitric acid aqueous solution as the electrolyte. In a two-electrode setup, as shown in Fig. 2(b), we connected the AlGaN samples as the anode, and a graphite rod served as the cathode. The n-contact was fully covered in the electrolyte during the P-ECE process. We applied a bias voltage ranging from 5 to 25 V to the system via a Keithley 2280 power source and illuminated the samples through the substrate. As the illumination source, we used 275, 265, and 255 nm LEDs and optical power densities varying between 0 and 23 mW/cm^2.

After the P-ECE experiments, we stripped the photoresist protection by soaking the samples in Remover 1165 (N-methyl-2-pyrrolidone) at 95 °C and then immersing them in isopropyl alcohol at room temperature. We exfoliated part of the membranes using carbon tape to measure the roughness of the etched N-polar surface by atomic force microscopy (AFM).

III. RESULTS AND DISCUSSION

Figure 3 shows the results from different illumination intensities using a 265 nm-LED after 5 min P-ECE at 15 V, for the sample with a 41%/51% sacrificial layer. Without exposure to UV light, there were no signs of etching [Figs. 3(a) and 3(e)]. For a UV illumination intensity of 9 mW/cm^2, part of the sacrificial layer was fully etched [Figs. 3(b) and 3(f)]. For higher illumination intensities, the etch front of complete etching (orange dotted line) extends further from the access hole (red dotted line), indicating a higher etch rate. In the light microscopy images, a second etching front is visible, which was identified as the porosification of the current-spreading layer, enclosed by the yellow dotted line. With increasing illumination, this porosification front also extends

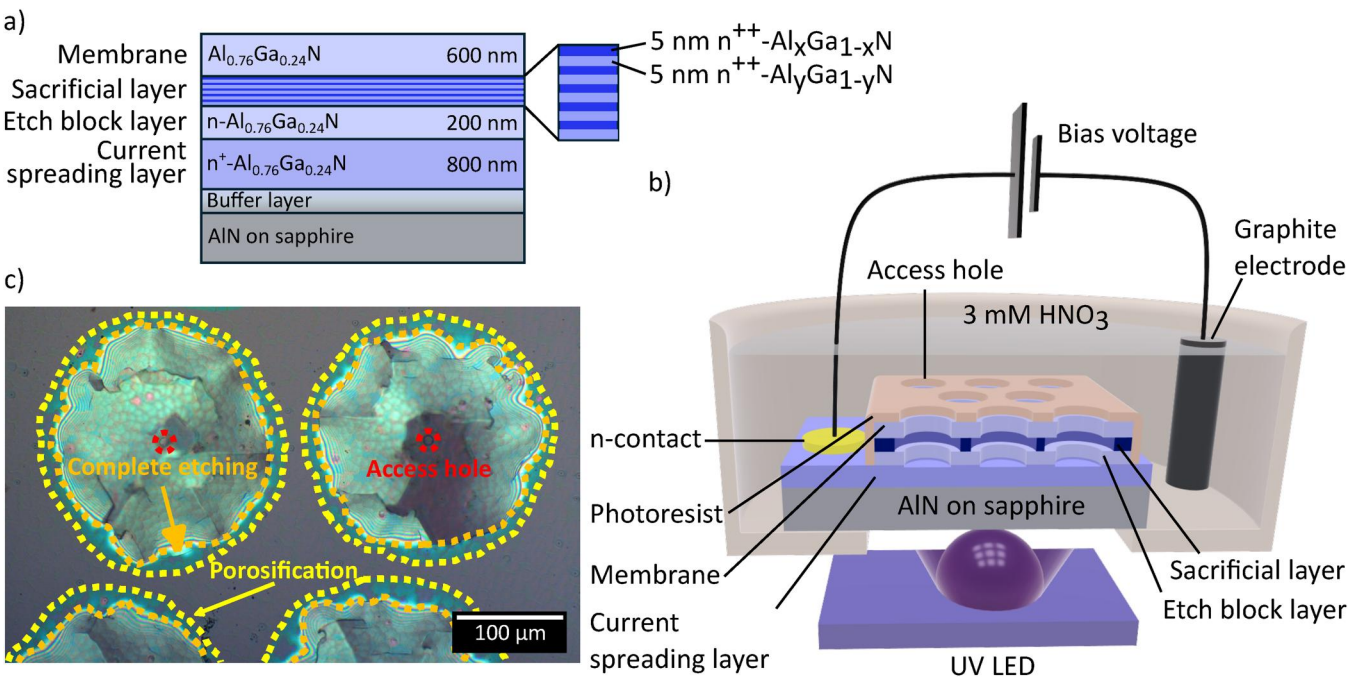

FIG. 2. (a) Epitaxial structure of the samples, (b) two-electrode setup used for photo-assisted electrochemical etching, and (c) top-view optical photography of the sample (41%/51%) after P-ECE at 15 V under 265 nm-LED illumination with an intensity of 23 mW/cm^2. The red dotted line indicates the dry-etched opening to expose the sacrificial layer; the orange dotted line indicates the etch front for complete etching of the sacrificial layer; and the yellow dotted line indicates the etch front for the porosification of the current-spreading layer. Note that the schematic dimensions in panel (b), including access-hole size and number, are not drawn to scale.

16 November 2026 08:04:57

© Author(s) 2026

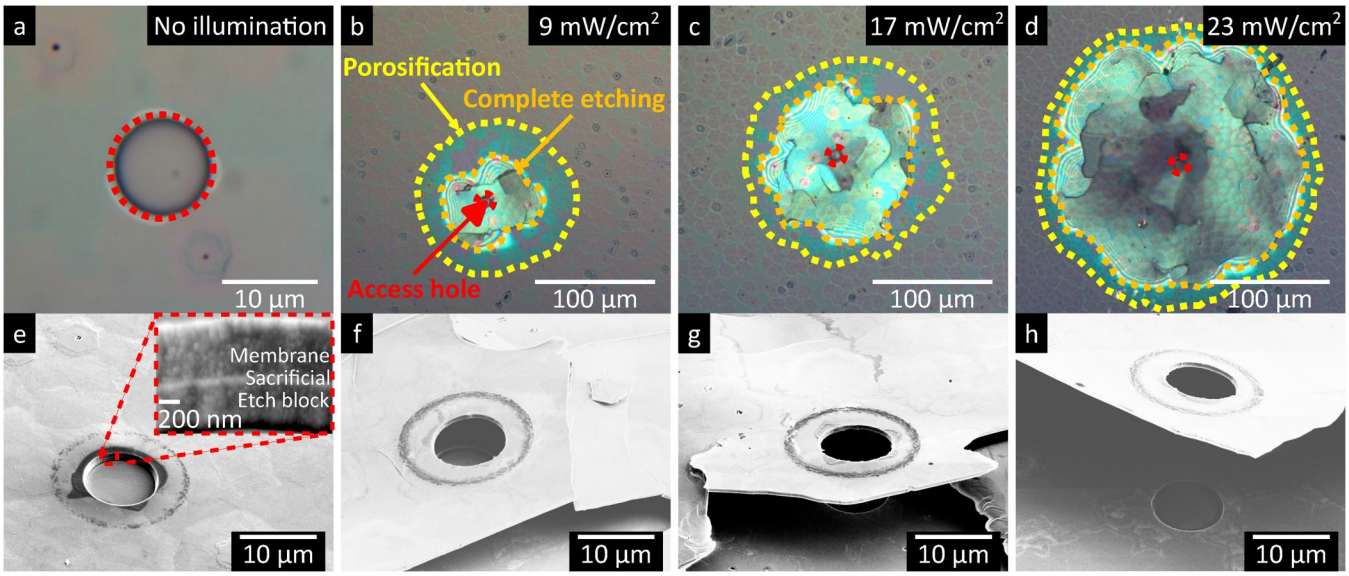

FIG. 3. (a)–(d) Optical microphotographs and (e)–(h) 45°-tilted SEM images of membranes on a sacrificial layer of (41%/51%) after P-ECE at 15 V under (a) and (e) no illumination, (b) and (f) 9, (c) and (g) 17, and (d) and (h) 23 mW/cm^2 of a 265 nm LED. The dotted red support line indicates the dry-etched opening to expose the sacrificial layer; the orange dotted line indicates the etch front for complete etching of the sacrificial layer; and the yellow dotted line indicates the etch front for the porosification of the current-spreading layer.

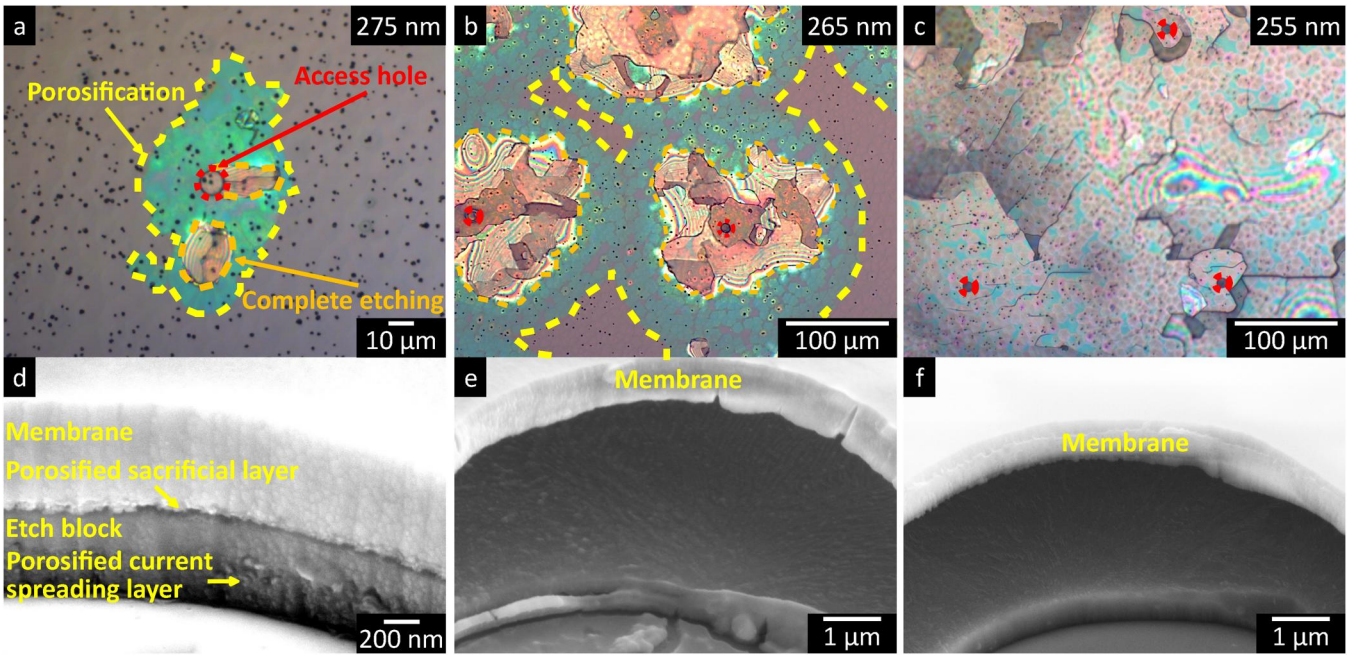

FIG. 4. (a)–(c) Optical microphotographs and (d)–(f) 45°-tilted SEM images of the (55%/65%) samples after P-ECE at a wavelength of (a) and (d) 275, (b) and (e) 265, and 255 nm (c) and (f) 255 nm. All experiments were conducted at 20 V for 20 min with an optical power density of 23 mW/cm^2. The red dotted support line indicates the dry-etched opening to expose the sacrificial layer; the orange dotted line indicates the etch front for complete etching of the sacrificial layer; and the yellow dotted line indicates the etch front for the porosification of the current-spreading layer.

16 November 2026 08:04:57

© Author(s) 2026

further from the access hole. The sacrificial layer complete-etching front approaches the current-spreading-layer porosification front with increasing illumination. The two almost align [Figs. 3(d) and 3(h)] at the highest illumination intensity tested (23 mW/cm^2). Thus, higher optical power densities increase the lateral etch rate of the sacrificial layer, which is estimated to be 7.9, 13.5, and 20.8 μm/min for 9, 17, and 23 mW/cm^2, respectively. Upon complete etching of the sacrificial layer, the mechanical connection between the membrane and the substrate is removed, allowing the membrane to relax toward its strain-free equilibrium state. As the AlGaN membrane structure is initially compressively strained to the underlying AlN buffer layer, the released membrane buckles upwards,[51,52] which can lead to cracking during the P-ECE process. Based on the radiation pattern of the LED in relation to the distance between the LED and the sacrificial layer, and the spatial extent of the hole array on the sample, the illumination intensity across the region to be etched was basically uniform. Despite the uniform illumination, some spatial variation in etching initiation was still observed, as shown in Fig. S2 in the supplementary material, and the origin of this remains elusive.

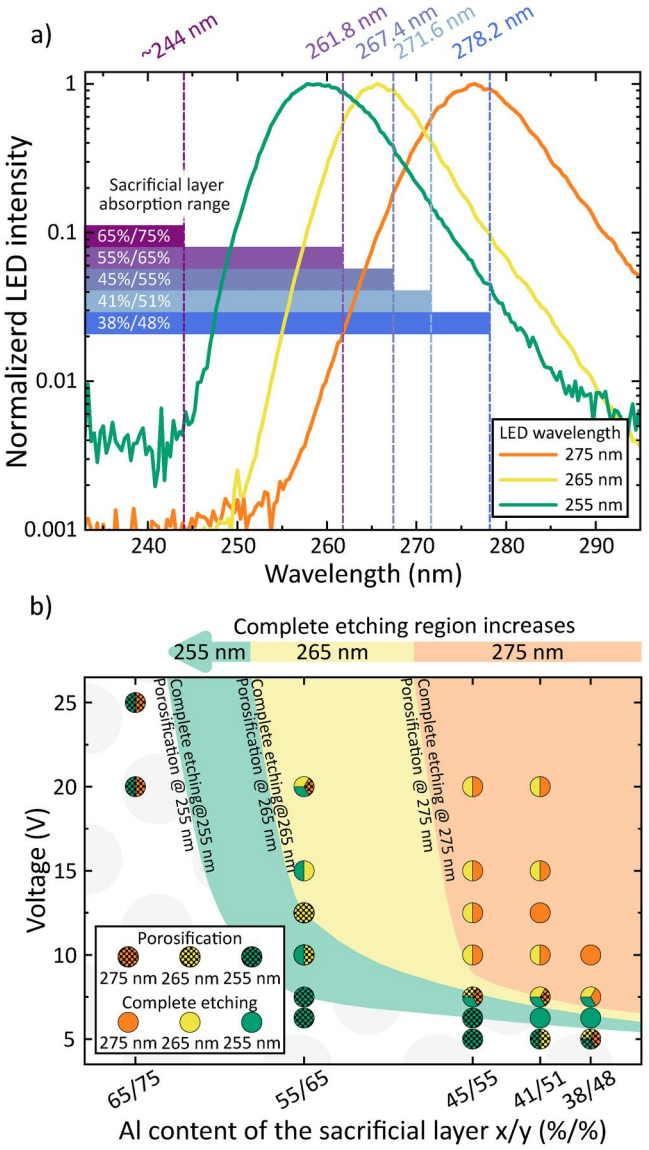

FIG. 5. (a) Measured LED spectra with inserted estimated absorption ranges of the sacrificial layers. The absorption edge was approximated as the photoluminescence peak wavelength. (b) Etching morphology related to the applied voltage, Al content (x/y) in the sacrificial layer, and LED illumination wavelength. All experiments were conducted with an optical power density of 23 mW/cm^2 for 20 min.

In the next step, we investigated the photo-assisted electrochemical etching (P-ECE) behavior of the (55%/65%) sample. This sample, which exhibited a photoluminescence (PL) peak of the sacrificial layer at 261.8 nm [see the PL measurement in Fig. S4 in the supplementary material and the estimated absorption range in Fig. 5(a)], was etched at 20 V bias voltage under illumination of 275, 265, and 255 nm LEDs with optical power density of 23 mW/cm^2 for 20 min. As shown in Figs. 4(a) and 4(d), illumination by the 275 nm LED mainly leads to the porosification of both the current spreader and the sacrificial layer. In contrast, the sacrificial layer was completely etched laterally when the process was run with the 265 and 255 nm LEDs, and membranes could be successfully lifted off. However, the membranes cracked as they were not free to expand when completely etched and relaxed. Under 255 nm photoexcitation, a higher lateral etch rate was achieved compared to 265 nm illumination after 20 min, as shown in Figs. 4(b) and 4(c), despite the slightly lower photon flux. This is likely due to the increased fraction of the 255 nm-LED spectrum, which is absorbed in the sacrificial layer [see Fig. 5(a)], leading to a higher density of photogenerated carriers available to drive the photoelectrochemical oxidation/dissolution reactions.[53] To examine changes in etching morphology with increasing distance from the access hole, the N-polar surface of the exfoliated 55%/65% sample corresponding to Fig. 4(b) was characterized by SEM near the access hole and approximately 100 μm away (Fig. S3 in the supplementary material). The dark spots in Figs. 4(a)–4(c) correspond to hillocks, which might originate from growth-related defects. Near the access hole, localized vertical etching was observed around some hillocks and merged with the main lateral etch front. Further from the access hole, the etch progressed more as desired, where the morphology indicates that the etch deflected around the hillocks without clear evidence of etching initiation starting at hillocks [Figs. S3(e) and S3(f) in the supplementary material]. The surface morphology associated with complete etching became increasingly aligned along the radial direction with increasing distance, but no clear transition from complete etching to porosification was observed within the inspected area.

In the following, we also extended the experiments to samples having sacrificial layers with Al mole fractions of (38%/48%), (41%/51%), (45%/55%), (55%/65%), and (65%/75%). Figure 5(a) shows the measured emission spectra of the 275, 265, and 255 nm LEDs, as well as the estimated absorption range of the sacrificial layers based on emission peaks from PL measurements (see Fig. S4 in the supplementary material). The etching results,

16 November 2026 08:04:57

© Author(s) 2026

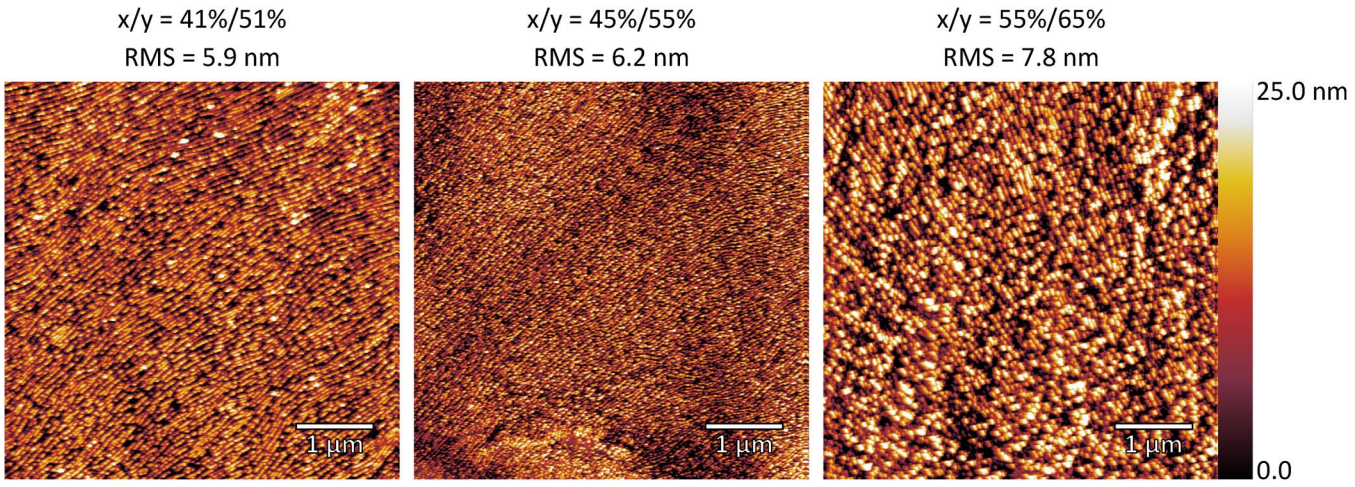

FIG. 6. AFM images of the exposed N-polar surface of the exfoliated membrane of the (41%/51%), (45%/55%), and (55%/65%) samples. The experiments were conducted at 15 V for 20 min, with an illumination intensity of 23 mW/cm^2 at 265 nm.

shown in Fig. 5(b), distinguish porosification and complete etching of the AlGaN sacrificial layers with varying Al contents under different applied voltages and illumination wavelengths. All experiments used 23 mW/cm^2 for 20 min. With higher Al content in the sacrificial layers, shorter excitation wavelengths are required to achieve complete etching due to the absorption edge shift.[54] Using a shorter-wavelength LED increases the spectral overlap between the LED emission spectrum and the sacrificial layer absorption range. As a result, more above-bandgap photons can be absorbed by the sacrificial layer, thereby generating more photoexcited carriers that promote complete etching. This is consistent with Fig. 4 for the (55%/65%) sacrificial layer, in which the estimated absorption onset overlaps the short-wavelength tail of the 265 and 255 nm emissions, while overlap with the 275 nm emission is limited [Fig. 5(a)]. The sample with the (65%/75%) sacrificial layer could only be porosified and not completely

16 November 2026 08:04:57

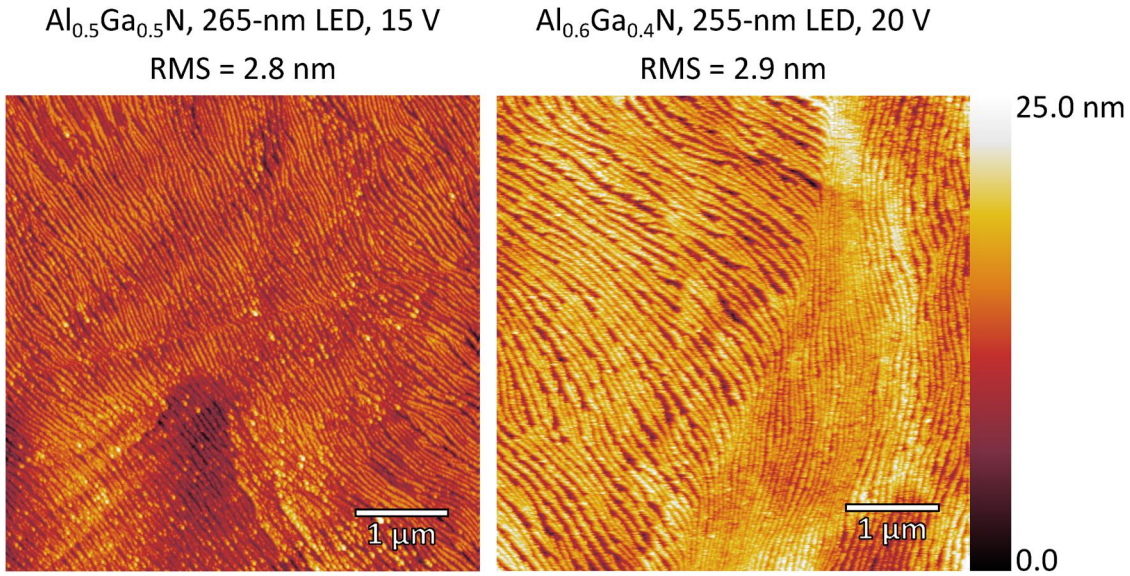

FIG. 7. AFM images of the N-polar surface of the exfoliated membrane after P-ECE of a 10 nm-thin sacrificial layer of $Al_{0.5}Ga_{0.5}N$ etched at 15 V under 265 nm-LED illumination and of $Al_{0.6}Ga_{0.4}N$ etched at 20 V under 255 nm-LED illumination. Both experiments were performed at an optical power density of 23 mW/cm^2.

© Author(s) 2026

etched, likely due to the low absorption of the light from the 265 and 255 nm LEDs. Complete etching of such a layer would require an even shorter excitation wavelength. The experiments in Fig. 5(b) also show that a shorter illumination wavelength reduced the required applied bias for complete etching.

In all our etching experiments, we did not observe any etching or porosification of the undoped membrane layer, confirming the very high selectivity and precise membrane thickness control. However, a low root-mean-square (RMS) roughness of the etched surface is also essential for many optical devices. We, therefore, examined the N-polar surface of the exfoliated membranes after P-ECE of the (41%/51%), (45%/55%), and (55%/65%) samples etched at 15 V under 265 nm illumination by AFM ($5 \times 5\,\mu m^2$, Fig. 6). The lifted-off membranes have RMS surface roughness values of 5.9 (41%/51%), 6.2 (45%/55%), and 7.8 nm (55%/65%), which are higher than those of the corresponding as-grown surfaces of 2.3, 3.2, and 2.6 nm, respectively. Detailed AFM profiles of the as-grown surfaces are provided in Fig. S6 in the supplementary material. The etched surfaces exhibit an elongated ripple pattern, indicating the lateral etch direction that depends on the orientation of the local electric field at the time of etching.[54] This ripple pattern also reveals details about the pore formation. When the pores widen, multiple pores branch off from the pore nucleus. However, when neighboring space-charge regions overlap and pore branching is inhibited, an unetched region remains.[54] We also observed slightly smoother RMS roughness of (41%/51%) and (45%/55%) samples compared to the (55%/65%) sample. As the Al content in the sacrificial layer increases, the bandgap increases, resulting in a decrease in electron affinity. This widens the space-charge region and reduces the potential drop across it, which, in turn, promotes the formation of smaller-sized pores with thicker walls during etching, thereby leading to a higher roughness.[44,55]

To reduce the roughness of the exfoliated membrane, we redesigned the sacrificial structure from a multilayer of total thickness of 50 nm to a 10 nm-thin single layer, since this would theoretically limit the pore height to a maximum of 10 nm (see Reducing the surface roughness section in the supplementary material). Figure 7 shows $5 \times 5\,\mu m^2$ AFM scans of N-polar etched surfaces of membranes grown on 10 nm-thin $Al_{0.5}Ga_{0.5}N$ and $Al_{0.6}Ga_{0.4}N$ sacrificial layers after P-ECE. The RMS roughness of the membranes released from 10 nm-thin $Al_{0.5}Ga_{0.5}N$ and $Al_{0.6}Ga_{0.4}N$ sacrificial layers is strongly reduced in comparison with the 50 nm multilayer sacrificial layer and is only slightly larger than that of the corresponding as-grown surfaces. The roughness increases from 2.1 nm as-grown to 2.8 nm after P-ECE for $Al_{0.5}Ga_{0.5}N$, and from 2.0 to 2.9 nm for $Al_{0.6}Ga_{0.4}N$ (see AFM images of as-grown top surfaces in Fig. S8 in the supplementary material). By reducing the sacrificial layer thickness, the surface roughness is considerably smoother after P-ECE; <3 nm RMS for the thin sacrificial layer vs 6–8 nm for the 50 nm sacrificial layer. This is promising; however, for a high-Al-content thin sacrificial layer (e.g., $Al_{0.6}Ga_{0.4}N$), the etch rate is substantially reduced, and etch initiation is more random, often starting at defects rather than in access holes (see Fig. S9 in the supplementary material). Thus, more investigations are needed to fully explore whether thin sacrificial layers could outperform multilayer sacrificial layers. In summary, not only the etch conditions but also the design of the sacrificial layer has a great influence on the final RMS roughness.

IV. CONCLUSIONS

We show the role of P-ECE process parameters on the etching of a high Al-containing AlGaN sacrificial layer and the final morphology of the exfoliated membranes. Shorter-wavelength illumination enhances complete lateral etching, and we achieved complete removal of the Al-rich multilayer AlGaN sacrificial layer with up to 65% Al content under 265 nm illumination, as well as with up to 55% Al content under 275 nm illumination. There is no sign of etching damage to the membrane in any P-ECE experiments, indicating highly selective removal of the sacrificial layer and reliable thickness control. For membranes released using multilayer AlGaN sacrificial layers, the N-polar surface roughness is in the range of 5.9–7.8 nm. Replacing the multilayer with a single 10 nm-thin AlGaN sacrificial layer leads to a smoother etched surface (2.8–2.9 nm) that is even comparable to that of the as-grown surface. Thus, P-ECE results in smoother etched surfaces compared to membrane surfaces achieved with other methods, such as mechanical thinning,[12] LLO,[14,33] and the WLO[20,22] without post-chemical treatment. We observed cracking during the P-ECE process due to membrane relaxation; therefore, strain engineering needs to be optimized when fabricating devices based on such membranes. Our results demonstrate that P-ECE is a promising method for realizing membrane-based AlGaN UV devices with high Al content, including thin-film flip-chip UVC LEDs and UVC VCSELs, as well as transferring them to a photonic integrated circuit.

SUPPLEMENTARY MATERIAL

The supplementary material contains the details of the fabrication flow, the uniformity of etch initiation under different illumination intensities, photoluminescence characterization, SEM observations of the photo-assisted electrochemical etching of AlGaN sacrificial layers, and SEM and AFM characterization of the N-polar membrane surfaces after lift-off.

ACKNOWLEDGMENTS

This work was performed in part at Myfab Chalmers, and it was financially supported by the European Union's Horizon Europe research and innovation program under Grant Agreement No. 101135845 (Qu-PIC), the European Research Council (ERC) under the European Union's Horizon 2020 research and innovation program (Grant Agreement No. 865622), and the Swedish Research Council (No. 2018-00295). The authors thank Silvia Hagedorn and Markus Weyers (FBH) for providing AlN/sapphire and Luna Hahn for operating and maintaining the MOVPE system at TU Berlin.

AUTHOR DECLARATIONS

Conflict of Interest

The authors have no conflicts to disclose.

16 November 2026 08:04:57

© Author(s) 2026

Author Contributions

Thanh Phuc Nguyen: Data curation (equal); Formal analysis (equal); Investigation (equal); Visualization (equal); Writing – original draft (equal); Writing – review & editing (equal). **Artem Shushanian**: Conceptualization (equal); Data curation (supporting); Formal analysis (supporting); Methodology (equal); Writing – original draft (equal); Writing – review & editing (equal). **Verena Kowallik**: Investigation (equal); Methodology (equal); Resources (equal); Writing – review & editing (equal). **Ryan Page**: Investigation (supporting). **Tim Wernicke**: Methodology (equal); Supervision (equal); Writing – review & editing (equal). **Michael Kneissl**: Funding acquisition (equal); Project administration (equal); Resources (lead); Supervision (lead); Writing – review & editing (equal). **Joachim Ciers**: Methodology (equal); Supervision (equal); Visualization (supporting); Writing – review & editing (equal). **Åsa Haglund**: Conceptualization (equal); Funding acquisition (lead); Project administration (lead); Resources (lead); Supervision (lead); Writing – review & editing (equal).

DATA AVAILABILITY

The data is available from the authors upon reasonable request.

REFERENCES

[1]E. Torres, J. Ciers, M. A. Bergmann, J. Höpfner, S. Graupeter, M. Grigoletto, M. Guttmann, T. Kolbe, T. Wernicke, M. Kneissl, and Å. Haglund, "Ultraviolet-B resonant-cavity light-emitting diodes with tunnel junctions and dielectric mirrors," ACS Photonics **11**(8), 2923–2929 (2024).

[2]Z. Zheng, Y. Mei, H. Long, J. Hoo, S. Guo, Q. Li, L. Ying, Z. Zheng, and B. Zhang, "AlGaN-based deep ultraviolet vertical-cavity surface-emitting laser," IEEE Electron Device Lett. **42**(3), 375–378 (2021).

[3]Z. Zheng, Y. Wang, J. Hoo, S. Guo, Y. Mei, H. Long, L. Ying, Z. Zheng, and B. Zhang, "High-quality AlGaN epitaxial structures and realization of UVC vertical-cavity surface-emitting lasers," Science China Materials **66**(5), 1978–1988 (2023).

[4]F. Hjort, J. Enslin, M. Cobet, M. A. Bergmann, J. Gustavsson, T. Kolbe, A. Knauer, F. Nippert, I. Häusler, M. R. Wagner, T. Wernicke, M. Kneissl, and Å. Haglund, "A 310 nm optically pumped AlGaN vertical-cavity surface-emitting laser," ACS Photonics **8**(1), 135–141 (2021).

[5]E. Torres, J. Ciers, N. Rebelo, F. Hjort, M. A. Bergmann, S. Graupeter, J. Enslin, G. Cardinalli, T. Wernicke, M. Kneissl, and Å. Haglund, "Ultraviolet-C vertical-cavity surface-emitting lasers with precise cavity length control," Laser Photonics Rev. **19**, 2402203 (2025).

[6]K. Kawasaki, C. Koike, Y. Aoyagi, and M. Takeuchi, "Vertical AlGaN deep ultraviolet light emitting diode emitting at 322 nm fabricated by the laser lift-off technique," Appl. Phys. Lett. **89**(26), 261114 (2006).

[7]L. Zhou, J. E. Epler, M. R. Krames, W. Goetz, M. Gherasimova, Z. Ren, J. Han, M. Kneissl, and N. M. Johnson, "Vertical injection thin-film AlGaN/AlGaN multiple-quantum-well deep ultraviolet light-emitting diodes," Appl. Phys. Lett. **89**(24), 241113 (2006).

[8]M. Takeuchi, T. Maegawa, H. Shimizu, S. Ooishi, T. Ohtsuka, and Y. Aoyagi, "AlN/AlGaN short-period superlattice sacrificial layers in laser lift-off for vertical-type AlGaN-based deep ultraviolet light emitting diodes," Appl. Phys. Lett. **94**(6), 061117 (2009).

[9]M. Shimokawa, Y. Yamada, T. Omori, K. Yamada, R. Hasegawa, T. Nishibayashi, A. Yabutani, S. Iwayama, T. Takeuchi, S. Kamiyama, M. Iwaya, H. Miyake, K. Miyoshi, K. Naniwae, and A. Yamaguchi, "Fabrication of vertical AlGaN-based deep-ultraviolet light-emitting diodes operating at high current density (~43 kA cm^{-2}) using a laser liftoff method," Appl. Phys. Express **15**(4), 041006 (2022).

[10]T. Nishibayashi, R. Kondo, E. Matsubara, R. Yamada, Y. Imoto, K. Hattori, S. Iwayama, T. Takeuchi, S. Kamiyama, H. Miyake, K. Naniwae, K. Miyoshi, A. Yamaguchi, and M. Iwaya, "Fabrication of vertical AlGaN-based ultraviolet-B laser diodes using a laser lift-off method," Appl. Phys. Express **16** (10), 104001 (2023).

[11]T. Nishibayashi, R. Kondo, E. Matsubara, R. Yamada, R. Miyake, Y. Sasaki, Y. Imoto, S. Iwayama, T. Takeuchi, S. Kamiyama, H. Miyake, and M. Iwaya, "Fabrication of vertical AlGaN-based ultraviolet-B laser diodes using a substrate exfoliation method with water," Phys. Status Solidi RRL **18**(11), 2300460 (2024).

[12]J. Yan, J. Yuan, Y. Jiang, H. Zhu, H. W. Choi, and Y. Wang, "A vertical AlGaN DUV light-emitting diode fabricated by wafer bonding and sapphire thinning technology," Appl. Phys. Express **15**(3), 032003 (2022).

[13]T. Kinoshita, K. Hironaka, T. Obata, T. Nagashima, R. Dalmau, R. Schlesser, B. Moody, J. Xie, S. Inoue, Y. Kumagai, A. Koukitu, and Z. Sitar, "Deep-ultraviolet light-emitting diodes fabricated on AlN substrates prepared by hydride vapor phase epitaxy," Appl. Phys. Express **5**(12), 122101 (2012).

[14]Z. Zheng, H. Long, S. Matta, M. Leroux, J. Brault, L. Ying, Z. Zheng, and B. Zhang, "Photoassisted chemical smoothing of AlGaN surface after laser lift-off," J. Vac. Sci. Technol. B **38**(4), 042207 (2020).

[15]B. K. SaifAddin, A. Almogbel, C. J. Zollner, H. Foronda, A. Alyamani, A. Albadri, M. Iza, S. Nakamura, S. P. DenBaars, and J. S. Speck, "Fabrication technology for high light-extraction ultraviolet thin-film flip-chip (UV TFFC) LEDs grown on SiC," Semicond. Sci. Technol. **34**(3), 035007 (2019).

[16]B. K. Saifaddin, M. Iza, H. Foronda, A. Almogbel, C. J. Zollner, F. Wu, A. Alyamani, A. Albadri, S. Nakamura, S. P. DenBaars, and J. S. Speck, "Impact of roughening density on the light extraction efficiency of thin-film flip-chip ultraviolet LEDs grown on SiC," Opt. Express **27**(16), A1074–A1083 (2019).

[17]H. Aoshima, K. Takeda, K. Takehara, S. Ito, M. Mori, M. Iwaya, T. Takeuchi, S. Kamiyama, I. Akasaki, and H. Amano, "Laser lift-off of AlN/sapphire for UV light-emitting diodes," Phys. Status Solidi C **9**(3–4), 753–756 (2012).

[18]F. Asif, H.-C. Chen, A. Coleman, M. Lachab, I. Ahmad, B. Zhang, Q. Fareed, V. Adivarahan, and A. Khan, "Substrate lifted-off AlGaN/AlGaN lateral conduction thin-film light-emitting diodes operating at 285 nm," Jpn. J. Appl. Phys. **52** (8S), 08JG14 (2013).

[19]K. Shojiki, M. Shimokawa, S. Iwayama, T. Omori, S. Teramura, A. Yamaguchi, M. Iwaya, T. Takeuchi, S. Kamiyama, and H. Miyake, "Centimeter-scale laser lift-off of an AlGaN UVB laser diode structure grown on nano-patterned AlN," Appl. Phys. Express **15**(5), 051004 (2022).

[20]E. Matsubara, R. Hasegawa, T. Nishibayashi, A. Yabutani, R. Yamada, Y. Imoto, R. Kondo, S. Iwayama, T. Takeuchi, S. Kamiyama, K. Shojiki, S. Kumagai, H. Miyake, and M. Iwaya, "A method for exfoliating AlGaN films from sapphire substrates using heated and pressurized water," Appl. Phys. Express **15**(11), 116502 (2022).

[21]R. Yamada, E. Matsubara, R. Kondo, T. Nishibayashi, K. Hattori, Y. Imoto, S. Iwayama, T. Takeuchi, S. Kamiyama, T. Maruyama, H. Miyake, and M. Iwaya, "Exfoliation mechanism of AlGaN-based thin films using heated-pressurized water," Appl. Phys. Express **16**(10), 105504 (2023).

[22]E. Matsubara, R. Yamada, R. Kondo, T. Nishibayashi, Y. Imoto, S. Iwayama, T. Takeuchi, S. Kamiyama, T. Maruyama, H. Miyake, S. Kobayashi, T. Yamamoto, and M. Iwaya, "Analysis of altered layers formed during substrate exfoliation of AlGaN crystals grown on periodic AlN nanopillars using the heated-pressurized water method," Phys. Status Solidi B **261**(11), 2300574 (2024).

[23]M. A. Bergmann, J. Enslin, R. Yapparov, F. Hjort, B. Wickman, S. Marcinkevičius, T. Wernicke, M. Kneissl, and Å. Haglund, "Electrochemical etching of AlGaN for the realization of thin-film devices," Appl. Phys. Lett. **115** (18), 182103 (2019).

[24]Q. Wu, Y. Guo, S. Sundaram, J. Yan, L. Zhang, T. Wei, X. Wei, J. Wang, A. Ougazzaden, and J. Li, "Exfoliation of AlN film using two-dimensional multilayer hexagonal BN for deep-ultraviolet light-emitting diodes," Appl. Phys. Express **12**(1), 015505 (2018).

16 November 2026 08:04:57

© Author(s) 2026

[25]Z. Chen, Z. Liu, T. Wei, S. Yang, Z. Dou, Y. Wang, H. Ci, H. Chang, Y. Qi, J. Yan, J. Wang, Y. Zhang, P. Gao, J. Li, and Z. Liu, "Improved epitaxy of AlN film for deep-ultraviolet light-emitting diodes enabled by graphene," Adv. Mater. **31**(23), 1807345 (2019).
[26]P. Wang, A. Pandey, J. Gim, W. J. Shin, E. T. Reid, D. A. Laleyan, Y. Sun, D. Zhang, Z. Liu, Z. Zhong, R. Hovden, and Z. Mi, "Graphene-assisted molecular beam epitaxy of AlN for AlGaN deep-ultraviolet light-emitting diodes," Appl. Phys. Lett. **116**(17), 171905 (2020).
[27]K. Okuno, S. Miura, M. Fujita, T. Takehisa, H. Muto, R. Oka, N. Hamashima, M. Ohya, Y. Saito, H. Ishiguro, T. Takeuchi, S. Kamiyama, and M. Iwaya, "Laser lift-off of ultraviolet-C light-emitting-diode epitaxial layers with an AlGaN nucleation layer grown on a sapphire substrate," Jpn. J. Appl. Phys. **64**(6), 065504 (2025).
[28]G. Cardinali, F. Hjort, N. Prokop, J. Enslin, M. Cobet, M. A. Bergmann, J. Gustavsson, J. Ciers, I. Häusler, T. Kolbe, T. Wernicke, Å. Haglund, and M. Kneissl, "Low-threshold AlGaN-based UVB VCSELs enabled by post-growth cavity detuning," Appl. Phys. Lett. **121**(10), 103501 (2022).
[29]W. Y. Fu and H. W. Choi, "Progress and prospects of III-nitride optoelectronic devices adopting lift-off processes," J. Appl. Phys. **132**(6), 060903 (2022).
[30]H. Yoshida, Y. Takagi, M. Kuwabara, H. Amano, and H. Kan, "Entirely crack-free ultraviolet GaN/AlGaN laser diodes grown on 2-in. Sapphire substrate," Jpn. J. Appl. Phys. **46**(9R), 5782–5784 (2007).
[31]J. Wang, C. Ji, J. Lang, F. Xu, L. Zhang, X. Kang, Z. Qin, X. Yang, N. Tang, X. Wang, W. Ge, and B. Shen, "Wafer-scale vertical injection III-nitride deep-ultraviolet light emitters," Nat. Commun. **15**(1), 9398 (2024).
[32]H. K. Cho, O. Krüger, A. Külberg, J. Rass, U. Zeimer, T. Kolbe, A. Knauer, S. Einfeldt, M. Weyers, and M. Kneissl, "Chip design for thin-film deep ultraviolet LEDs fabricated by laser lift-off of the sapphire substrate," Semicond. Sci. Technol. **32**(12), 12LT01 (2017).
[33]Z. Zheng, Y. Li, O. Paul, H. Long, S. Matta, M. Leroux, J. Brault, L. Ying, Z. Zheng, and B. Zhang, "Loss analysis in nitride deep ultraviolet planar cavity," J. Nanophotonics **12**(04), 1 (2018).
[34]J. T. Leonard, D. A. Cohen, B. P. Yonkee, R. M. Farrell, S. P. DenBaars, J. S. Speck, and S. Nakamura, "Smooth e-beam-deposited tin-doped indium oxide for III-nitride vertical-cavity surface-emitting laser intracavity contacts," J. Appl. Phys. **118**(14), 145304 (2015).
[35]M. A. Bergmann, J. Enslin, M. Guttmann, L. Sulmoni, N. L. Ploch, F. Hjort, T. Kolbe, T. Wernicke, M. Kneissl, and Å. Haglund, "Increased light extraction of thin-film flip-chip UVB LEDs by surface texturing," ACS Photonics **10**(2), 368–373 (2023).
[36]M. A. Bergmann, J. Enslin, F. Hjort, T. Wernicke, M. Kneissl, and Å. Haglund, "Thin-film flip-chip UVB LEDs realized by electrochemical etching," Appl. Phys. Lett. **116**(12), 121101 (2020).
[37]T.-H. Chang, K. Xiong, S. H. Park, G. Yuan, Z. Ma, and J. Han, "Strain-balanced AlGaN/GaN/AlGaN nanomembrane HEMTs," Sci. Rep. **7**(1), 6360 (2017).
[38]A. W. Bruch, K. Xiong, H. Jung, X. Guo, C. Zhang, J. Han, and H. X. Tang, "Electrochemically sliced low loss AlGaN optical microresonators," Appl. Phys. Lett. **110**(2), 021111 (2017).
[39]Y. Yang, X. Wang, L. Zhang, and S. Wu, "High-performance UV detector based on freestanding AlGaN film by electrochemical etching technology," Proc. SPIE **13548**, 135480T (2025).
[40]Y. Zhang, S.-W. Ryu, C. Yerino, B. Leung, Q. Sun, Q. Song, H. Cao, and J. Han, "A conductivity-based selective etching for next-generation GaN devices," Phys. Status Solidi B **247**(7), 1713–1716 (2010).
[41]M. Sawicka, N. Fiuczek, H. Turski, G. Muziol, M. Siekacz, K. Nowakowski-Szkudlarek, A. Feduniewicz-Żmuda, P. Wolny, and C. Skierbiszewski, "Revealing inhomogeneous Si incorporation into GaN at the nanometer scale by electrochemical etching," Nanoscale **12**(10), 6137–6143 (2020).
[42]K.-C. Wu, K.-P. Huang, P.-F. Cheng, W.-P. Tseng, Y.-C. Huang, R.-H. Jiang, J.-H. Wang, B.-C. Shieh, C.-F. Lai, and C.-F. Lin, "Fabricated InGaN membranes through a wet lateral etching process," Appl. Phys. Express **6**(8), 086501 (2013).
[43]D. Chen, "Nanoscale manipulation of GaN for next-generation devices via electrochemical etch," Ph.D. thesis (Yale University, 2016).
[44]P. H. Griffin and R. A. Oliver, "Porous nitride semiconductors reviewed," J. Phys. D: Appl. Phys. **53**(38), 383002 (2020).
[45]R. Dalmau, B. Moody, R. Schlesser, S. Mita, J. Xie, M. Feneberg, B. Neuschl, K. Thonke, R. Collazo, A. Rice, J. Tweedie, and Z. Sitar, "Growth and characterization of AlN and AlGaN epitaxial films on AlN single-crystal substrates," J. Electrochem. Soc. **158**(5), H530–H535 (2011).
[46]H. Miyake, G. Nishio, S. Suzuki, K. Hiramatsu, H. Fukuyama, J. Kaur, and N. Kuwano, "Annealing of an AlN buffer layer in N_2–CO for growth of a high-quality AlN film on sapphire," Appl. Phys. Express **9**(2), 025501 (2016).
[47]E. Torres, "Ultraviolet AlGaN-based microcavities," Ph.D. thesis (Chalmers University of Technology, Gothenburg, 2025).
[48]Z. Shaban, V. Z. Zubialevich, E. A. Amargianitakis, F. B. Atar, P. J. Parbrook, Z. Li, and B. Corbett, "Ingan/AlInN interface with enhanced holes to improve photoelectrochemical etching and GaN device release," Semicond. Sci. Technol. **38**(5), 055015 (2023).
[49]M. S. Minsky, M. White, and E. L. Hu, "Room-temperature photoenhanced wet etching of GaN," Appl. Phys. Lett. **68**(11), 1531–1533 (1996).
[50]T. Sato, M. Toguchi, Y. Komatsu, and K. Uemura, "Low-damage etching for AlGaN/GaN HEMTs using photo-electrochemical reactions," IEEE Trans. Semicond. Manuf. **32**(4), 483–488 (2019).
[51]E. Zaus, M. Hermann, M. Stutzmann, and M. Eickhoff, "Fabrication of free-standing GaN microstructures using AlN sacrificial layers," Phys. Status Solidi RRL **1**(1), R10–R12 (2007).
[52]R. Kawakami, M. Niibe, Y. Nakano, S.-i. Yanagiya, Y. Yoshitani, C. Azuma, and T. Mukai, "Effects of ultraviolet wavelength and intensity on AlGaN thin film surfaces irradiated simultaneously with CF_4 plasma and ultraviolet," Vacuum **159**, 45–50 (2019).
[53]D. Brunner, H. Angerer, E. Bustarret, F. Freudenberg, R. Höpler, R. Dimitrov, O. Ambacher, and M. Stutzmann, "Optical constants of epitaxial AlGaN films and their temperature dependence," J. Appl. Phys. **82**(10), 5090–5096 (1997).
[54]M. J. Schwab, D. Chen, J. Han, and L. D. Pfefferle, "Aligned mesopore arrays in GaN by anodic etching and photoelectrochemical surface etching," J. Phys. Chem. C **117**(33), 16890–16895 (2013).
[55]M. Pophristic, S. P. Guo, and B. Peres, "High-conductivity n-AlGaN with high Al mole fraction grown by metalorganic vapor phase deposition," Appl. Phys. Lett. **82**(24), 4289–4291 (2003).

16 November 2026 08:04:57

© Author(s) 2026